Steric *vs.* electronic anomaly observed from iodomethane oxidative addition to tertiary phosphine modified rhodium(I) acetylacetonato complexes following progressive phenyl replacement by cyclohexyl [PR_3 = PPh_3, PPh_2Cy, $PPhCy_2$ and PCy_3]†

Alice Brink, Andreas Roodt,* Gideon Steyl and Hendrik G. Visser*

Received 22nd October 2009, Accepted 23rd April 2010
First published as an Advance Article on the web 17th May 2010
DOI: 10.1039/b922083f

Rhodium(I) acetylacetonato complexes of the formula [Rh(acac)(CO)(PR_3)] [acac = acetylacetonate, PR_3 = PPh_3 **1**, $PCyPh_2$ **2**, PCy_2Ph **3**, PCy_3 **4**] were synthesized and the iodomethane oxidative addition to these complexes were studied. Spectroscopic and low temperature (100 K) single crystal X-ray crystallographic data of the rhodium complexes (**1–4**) indicate a systematic increase in both steric and electronic parameters of the phosphine ligands as phenyl groups on the tertiary phosphine are progressively replaced by cyclohexyl groups in the series. Second order rate constants for the alkyl formation in the oxidative addition of iodomethane in dichloromethane at 25 °C vary with approximately one order-of-magnitude from $6.98(6) \times 10^{-3}$ $M^{-1}s^{-1}$ ($PCyPh_2$ **2**) to $55(1) \times 10^{-3}$ M^{-1} s^{-1} (PCy_2Ph **3**) and do not follow the expected electronic pattern from **1** to **4**, which indicates a flexibility of the cyclohexyl group, significantly influencing the reactivity. Activation parameters for the reactions range from 35(3) to 44(1) kJ mol^{-1} for $\Delta H^{\neq}$ and −140(5) to −154(9) J K^{-1} mol^{-1} for $\Delta S^{\neq}$, and are supporting evidence for an associative activation for the oxidative addition step.

Introduction

The rhodium- and iodide-catalysed process for the carbonylation of methanol to produce acetic acid was developed in the late sixties by the Monsanto company.[1] To date, it is still one of the most successful industrial applications of homogeneous catalysis and produces several million tons of acetic acid per year. The iodomethane oxidative addition reaction is the rate-determining step of the catalytic cycle and a desire to obtain a faster catalyst by substituting a carbonyl ligand in $[Rh(CO)_2I_2]^-$ with a more electron-donating ligand, such as phosphines, is often expressed.[2]

The manipulation of the reactivity of the Rh(I) metal centre in [Rh(BID)(CO)(PR_3)] type of complexes (BID = different monocharged O,O; N,O; O,S and N,S donor atom bidentate ligands[3–6] PR_3 = different monodentate tertiary phosphine ligands) in oxidative addition reactions has been reported previously. The rates of these reactions are influenced by the steric and electronic parameters of the non-participating ligands. Large, sterically demanding ligands bonded to the Rh(I) metal centre can inhibit the ease of the iodomethane moiety entering the rhodium co-ordination sphere and decrease the catalytic activity, while ligands with strong electron-donating abilities enhance the rates of these reactions.[2,3,5]

Over the years, numerous studies have been undertaken to investigate the formation of various products in the oxidative addition reactions between iodomethane and [Rh(BID)(CO)(PR_3)].[3,4,7–10] Both the *cis* and *trans* addition products of iodomethane on the rhodium metal centre have been isolated. [RhI(cupf)(CO)(CH_3)(PPh_3)][8] formed the *cis* addition product while [RhI(OX)(CO)(CH_3)(PPh_3)][4] formed the *trans* alkyl species. When the bidentate ligand contained a sulfur atom, as in the case of [Rh(Sacac)(CO)(PPh_3)],[9,10] the primary product reported was an acyl species. In this case the rate at which the Rh(I) complex disappeared was equal to the formation of the acyl species. It was later shown that the same mechanism is operative;[11] the process being significantly influenced by the steric properties induced by the bidentate ligand.[5] The oxidative addition of iodomethane to **1** has previously been reported by Basson *et al.*[3] and the spectral characteristics discussed by Varshavsky *et al.*[7]

Although different bidentate and phosphine ligand variations were reported during the past two decades as presented above,[5,6,12] the stepwise interchange of phenyl for cyclohexyl groups has not been studied to date. Thus, we report here the oxidative addition of iodomethane to [Rh(acac)(CO)(PR_3)] (acac = acetylacetonate) complexes by systematically manipulating the steric and electronic parameters of the phosphorous ligands in a series of phosphines ranging from triphenylphosphine (PPh_3) to tricyclohexylphosphine (PCy_3) (Fig. 1).

Acetylacetonate was selected as symmetric bidentate ligand to ensure the minimum number of isomers present during the reaction process.

Crystallographic determinations of the [Rh(acac)(CO)(PR_3)] complexes with PR_3 = PPh_3 and PCy_3 have been reported before by Leipoldt *et al.*[13] and Trzeciak *et al.*[14] Recently, we also reported

Department of Chemistry, University of the Free State, P.O. Box 339, Bloemfontein, 9300, South Africa. E-mail: roodta@ufs.ac.za; Fax: +27 (0)51 4446384; Tel: +27 (0)51 401 2547

† Electronic supplementary information (ESI) available: Additional tables and figures. CCDC reference numbers 752115 and 752116. For ESI and crystallographic data in CIF or other electronic format see DOI: 10.1039/b922083f

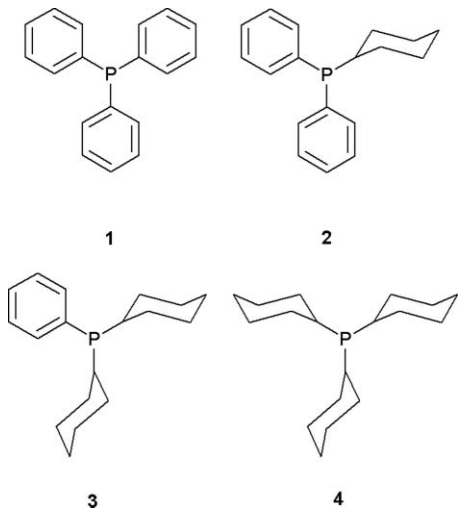

Fig. 1 Monodentate tertiary phosphine ligands utilized in [Rh(acac)-(CO)(PR_3)] for complexes **1** to **4**.

the crystal structures of the complexes of **2** and **3**,[15,16] but to ensure a proper solid state comparison, all four the complexes' structures were redetermined at low temperature to carefully evaluate bond length changes. These crystallographic results are also briefly reported here.

Results and discussion

Synthesis

The tertiary phosphine series PPh_3, $PCyPh_2$, PCy_2Ph and PCy_3 react with [Rh(acac)$(CO)_2$] in a similar way as previously reported,[17,18] and rapid substitution of the first CO ligand occurs. High yields were obtained with the synthesis of the [Rh(acac)(CO)(PR_3)] complexes, using octane as a solvent. The use of acetone as a solvent, with regards to complexes **2** and **3**, resulted in decomposition to an oil except when synthesized under Schlenk conditions.

IR spectra

Infrared data for **1** to **4** were recorded in both the solid and solution state and are presented in Table 1. The carbonyl stretching frequencies, ν(CO), decrease (1977.6 cm^{-1} to 1945.3 cm^{-1}) for complexes **1** to **4**, indicating the expected systematic increase in electron density on the rhodium(I) metal centre (increased d-π backbonding) ability as the phenyl is stepwise replaced by cyclohexyl.

Table 1 Summary of spectroscopic data for [Rh(acac)(CO)(PR_3)] complexes

	PR_3	(**1**)	(**2**)	(**3**)	(**4**)
IR	ν**(CO)/cm^{-1}**[a]	1977.6	1959.3	1948.8	1945.3
	ν**(CO)/cm^{-1}**[b]	1977.0	1971.2	1967.4	1959.7
^{31}P NMR	δ **(ppm)**	48.6	53.3	58.8	59.3
	$^1J_{Rh-P}$**/Hz**	177.0	171.3	168.3	164.3

[a] Neat samples, ATR. [b] In CH_2Cl_2.

The use of IR spectroscopy in determining the electron-donor ability of phosphorous ligands have been illustrated with a variety of phosphite and phosphine rhodium and iridium complexes. Phosphite ligands, such as $P(OPh)_3$ are known as better π-acceptors and poorer σ-donors compared to PPh_3.[17,22] The ν(CO) value of [Rh(β-diketonato)(CO)($P(OPh)_3$)] is observed around 2000 cm^{-1}, while the values of analogous phosphine complexes[17] are found at about 1970 cm^{-1}. The use of even stronger π-acceptor ligands[18,19] such as $P(NC_4H_4)_3$, increases the ν(CO) frequency even further to 2012 cm^{-1}. The weaker σ-donor and better π-acceptor properties of $P(OPh)_3$ may be further illustrated by the formation of [Rh(β-diketonato)($P(OPh)_3)_2$] complexes. Both CO groups of [Rh(β-diketonato)$(CO)_2$] complexes may be substituted by $P(OPh)_3$ due to the weakened Rh–C bond in the [Rh(β-diketonato)(CO)($P(OPh)_3$)] complexes[17,18] and since $P(OPh)_3$ has much less steric demand than PPh_3, it allows the Rh(I) metal centre to more easily accommodate two $P(OPh)_3$ ligands in this fashion.

NMR spectra

^{31}P-NMR spectra of all the complexes were obtained in dichloromethane at 25.0 °C. The value of the coupling constant, δ, increases systematically from complex **1** to **4** (Table 1), whereas the $^1J_{Rh-P}$ shows a corresponding decrease. The value of $^1J_{Rh-P}$, according to the Fermi contact term, is very sensitive to changes in the overlap between the 5s(Rh)-3s(P) orbitals.[5] The decreasing $^1J_{Rh-P}$ value suggests that the overlap between the orbitals decrease and the Rh–P bond distance will increase with the gradual substitution of a phenyl group by a more spatially demanding cyclohexyl ring.[6]

The ^{31}P-NMR data, together with the IR results thus clearly show that the systematic replacement of a phenyl group by a cyclohexyl group increases the electron-density on the metal centre for the systematic progression from **1** to **4**.

X-ray crystallography

The crystal structures for **1** to **4** were determined at 100 K and the basic data collection parameters are reported in the *S. Table 1* (see electronic supplementary information, ESI).† The steric demand of the phosphine ligands in this study, was quantified by the effective Tolman cone angle (θ_E), using the actual Rh–P bond distance.[20] A van der Waals radius of 1.2 Å for hydrogen and C–H bond distances of 0.97 Å for CH_2 and 0.93 Å for CH were used. In solution, the ligand substituents orientation might differ, resulting in a variation in cone angle size.[21] The effective cone angles (θ_E), all indicate an expected increase in steric demand of the phosphine ligands from **1** to **4** (Table 2). The θ_E values of 149.3 and 169.5° for PPh_3 and PCy_3 ligands correspond well to the published Tolman[22] cone angles, θ_T, of 145 and 170°, determined according to the definition using a Ni–P bond distance of 2.28 Å.

Table 2 Selected structural properties of [Rh(acac)(CO)(PR_3)]

PR_3	Effective Cone angle, θ_E/°	Rh–P/Å	Rh-O2/Å	C1-O1/Å
(**1**)	149.3	2.2418(9)	2.0747(16)	1.153(3)
(**2**)	151.2	2.2327(6)	2.0764(17)	1.149(4)
(**3**)	163.5	2.2425(9)	2.0788(16)	1.151(3)
(**4**)	169.5	2.2537(4)	2.0879(10)	1.157(2)

The calculated density of the reported structures decrease systematically from 1.565 to 1.400 g cm^{-1} from **1** to **4** and confirms further, a progressive increase in overall spatial occupation in the unit cell and asymmetric unit as the ligand size increases. This is further manifested in the increase in volume of the asymmetric unit; = [(unit cell volume)/Z], from 523, 557, 587, to 606 Å^3, for PPh_3, $PCyPh_2$, PCy_2Ph and PCy_3, respectively (*S.Table 1*†).

The Rh-O2 bond distances increase, although not strictly systematically, from complex **1** to **4** (Fig. 2, Table 2), indicating the increase in the *trans* influence of the phosphine ligands with the increase in steric demand. The Rh–P bond distance varies between 2.2418(9) and 2.2537(4) Å, and the C≡O bond distance between 1.149(4) and 1.157(2) Å. The rest of the crystallographic results from the crystal structure data, *i.e.* Rh–P and C≡O bond distances, do not show the same systematic tendencies as were observed with the IR and ^{31}P-NMR spectroscopy. This could be ascribed to packing effects and hydrogen bonding interactions.[15,16] It is however interesting to note that the Rh–P bond distance in [Rh(acac)(CO)(**PCyPh$_2$**)] is the shortest at 2.2327(6) Å of the four complexes **1–4**, potentially supporting an electron rich rhodium(I) centre.

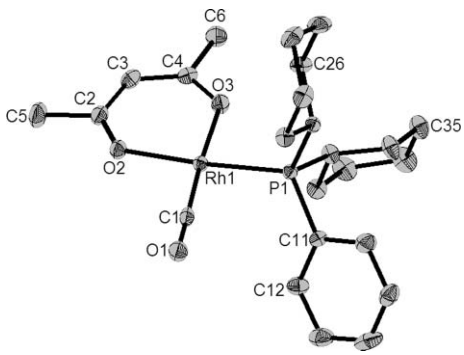

Fig. 2 Atom numbering scheme for crystallographic data of [Rh(acac)(CO)(PR$_3$)] complexes as indicated by complex **3**.

Kinetics

The kinetic results of the four [Rh(acac)(CO)(PR$_3$)] complexes were surprisingly different. The formation of the expected Rh(III)-alkyl^I species for the four [Rh(acac)(CO)(PR$_3$)] complexes were observed with all the spectroscopic methods reported. However, after this first step, the reactions proceed *via* slightly different pathways (*S.Fig. 1*†).

The oxidative addition of CH_3I, as determined by IR and ^{31}P NMR, to [Rh(acac)(CO)(**PPh$_3$**)] (1977.6 cm^{-1}) (Fig. 3 and 4) resulted in the rapid formation of an alkyl^I product (2071.5 cm^{-1}; 32.8 ppm), followed by a slower reaction attributed to acyl formation (1720.5 cm^{-1}, 37.7 ppm). As the alkyl^I started to disappear, the acyl was still increasing to a maximum absorbance. ^{31}P NMR scans of the same reaction indicated that after acyl formation (37.7 ppm), a Rh(III)-alkyl^{II} (29.5 ppm) slowly began to form after *ca*. 28 min; this was not observed by the IR spectra.

The geometry of these two alkyl species cannot be unequivocally defined nor concluded from the current NMR spectra. However, all solid state structures of reactants and products to date suggest that the carbonyl ligand always lies in the equatorial plane

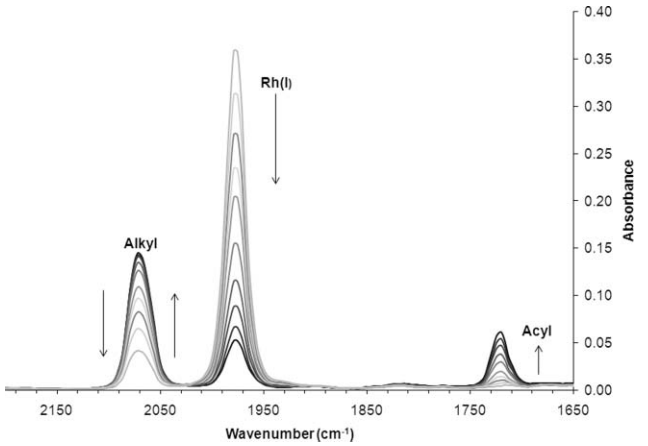

Fig. 3 Infrared spectral changes observed during oxidative addition of MeI to [Rh(acac)(CO)(PPh$_3$)] in CH_2Cl_2. Spectra indicate the disappearance of Rh(I) species with simultaneous increase of the alkyl^I peak. The acyl peak formation corresponds to the disappearance of the alkyl^I species. [Rh(acac)(CO)(PPh$_3$)] = 3.12×10^{-3} M, [CH_3I] = 0.165 M, Δt = 16.5 s, $k_{obs} = 6.20(9) \times 10^{-3}$ s^{-1}.

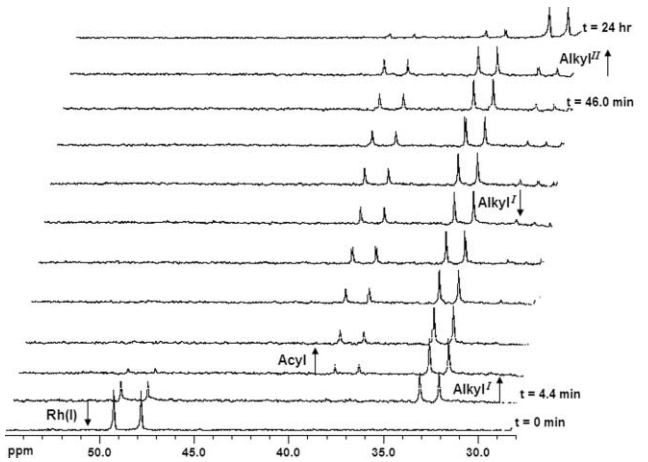

Fig. 4 Observed ^{31}P-NMR spectra for the disappearance of the four co-ordinated [Rh(acac)(CO)(PPh$_3$)] species and the formation of the alkyl^I, acyl and alkyl^{II} intermediate products in CH_2Cl_2. [Rh(acac)(CO)(PPh$_3$)] = 3.583×10^{-2} M, [CH_3I] = 0.156 M, Δt = 3 min, $k_{obs} = 5.3(8) \times 10^{-3}$ s^{-1}.

as defined by the bidentate ligand, and *trans* to one of the bidentate ligand (O,O for acac types or O,N for Schiff base types) donor atoms, with the iodido ligand in the apical position.[8,12,23–29] Moreover, this solid state data indicate that the P-donor ligand and the methyl group sometimes switch positions, as expected for either a *cis* (*via* a concerted three-centred process) or a *trans* (*via* a linear transition state/ionic process) oxidative addition reaction. This observed positional interchange as observed in the thermodynamic ground state structures, might be either due to the mode of initial coordination or subsequent formal isomerisation *via e.g.* an acyl species. Although there are significant changes in the *chemical shift* values of the Rh(III)-alkyl^I and Rh(III)-alkyl^{II} species in this study, the $^1J_{Rh-P}$ values differ only by approximately 3–6 Hz, see *S.Table 2*.† This suggests the exclusion of a *trans* CH_3–Rh–P orientation in the alkyl species in this study observed

by ^{31}P NMR, since the methyl group has a much larger *trans* influence than an oxygen donor atom from the acac backbone or an iodido ligand. This will most probably result in a smaller $^{1}J_{Rh-P}$ than the *ca.* 116–124 Hz for all the species found in this study.[5,6] Furthermore, the conversion from alkyl^{I} to finally alkyl^{II} suggests moving to a more thermodynamic stable state and thus a lower energy for alkyl^{II}, in agreement with preliminary computational studies,[30,31] which showed a *ca.* 10 to 28 kJ mol^{-1} energy difference between the geometry of the Rh(III)-alkyl^{I} compared to that of the Rh(III)-alkyl^{II}, as depicted in Fig. 6. However, it must again be noted from these preliminary computational studies that seemingly small steric differences may have a significant influence on relative distributions of species. The complete computational study is underway, but for the purpose of this paper, the geometries for Rh(III)-alkyl^{I} (apical *trans* I–Rh-CH_3 orientation) and Rh(III)-alkyl^{II} (apical *trans* I–Rh–P orientation) are assumed as indicated in Fig. 6.

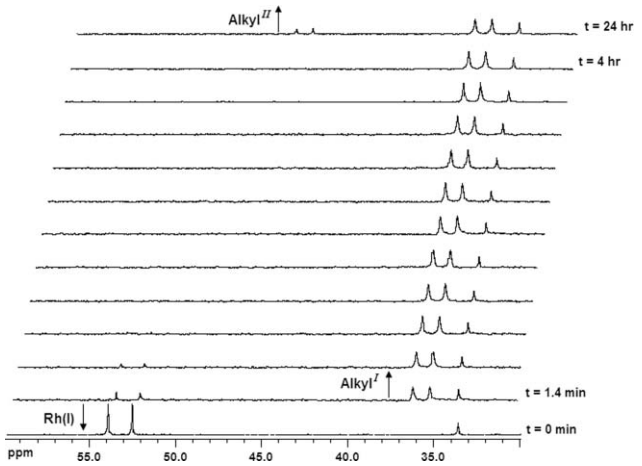

Fig. 5 Observed ^{31}P-NMR spectra for the disappearance of the four co-ordinated [Rh(acac)(CO)(PCyPh$_2$)] species and the formation of the alkyl^{I} and alkyl^{II} products in CH_2Cl_2 at 25 °C. Free phosphine, PCyPh$_2$ was added as an internal standard at 33.6 ppm. [Rh(acac)(CO)(PCyPh$_2$)] = 3.44×10^{-2} M, [CH_3I] = 0.156 M, $\Delta t = 0.9$ min, $k_{obs} = 9.7(5) \times 10^{-3}$ s^{-1}.

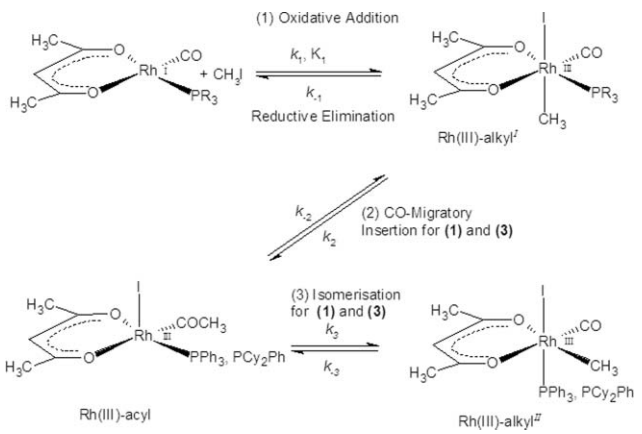

Fig. 6 General simplified reaction scheme for the iodomethane oxidative addition to complexes (**1**) and (**3**).

IR spectra for the oxidative addition of CH_3I to [Rh(acac)(CO)(**PCyPh$_2$**)], on the other hand, indicated the formation of an alkyl^{I} species (2067.7 cm^{-1}; 35.8 ppm) which was not succeeded by acyl formation (Fig. 5). NMR spectra showed the formation of an alkyl^{II} species (46.3 ppm) after 24 h. No acyl species formation occurred during this time period.

The reaction of [Rh(acac)(CO)(**PCy$_2$Ph**)] indicated the slow formation of an alkyl^{I} intermediate (2052.3 cm^{-1}; 43.0 ppm) followed by an even slower forming acyl species after *ca.* 37 min (38.1 ppm). After 3 h another alkyl species attributed to a Rh(III)-alkyl^{II} isomer (41.7 ppm) was observed (Fig. 6).

The observed data for the reaction of [Rh(acac)(CO)(**PCy$_3$**)] with CH_3I suggests the formation of an alkyl^{I} intermediate (2052.3 cm^{-1}; 50.2 ppm) followed by the formation of a second alkyl^{II} isomer (45.0 ppm) after 12 min, and then the formation of an acyl species (40.2 ppm) after 28 min. (*S.Fig. 1*†)

The oxidative addition of iodomethane to Rh(I) complexes proceed in general as an equilibrium reaction, confirmed by Roodt *et al.*[5] At low iodomethane concentrations a small amount of alkyl^{I} is formed from the Rh(I) reactant, while at higher [CH_3I], more of the alkyl^{I} species is formed and at a much faster rate.

Plots of the observed first-order rate constants (k_{obs}) *versus* iodomethane concentrations, for the oxidative addition to the [Rh(acac)(CO)(PR$_3$)] complexes, yielded linear relationships with non-zero intercepts for the tertiary phospine series. A typical example of such a plot for the formation of the alkyl^{I} species for complex **3** is shown in Fig. 7. Similar plots were obtained for the other PR$_3$ complexes. (*S.Fig. 2–4*†)

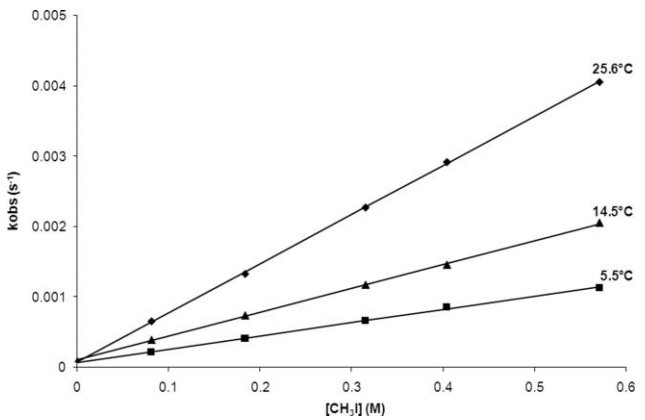

Fig. 7 Temperature and [CH_3I] dependence of the pseudo-first order rate constant for the formation of [Rh(acac)I(CH_3)(CO)(PCy$_2$Ph)] in dichloromethane, UV/vis; ($\lambda = 323$ nm) [Rh(acac)(CO)(PCy$_2$Ph)] = 9.10×10^{-5} M.

The solid lines represent the least-squares fits of the k_{obs} data *versus* [CH_3I] at three different temperatures. The results are consistent with the following rate expression of a simple two step reversible reaction (Fig. 6):[5,11]

$$k_{obs} = k_1[CH_3I] + k_{-1} \quad (1)$$

where k_1 and k_{-1} are the rate constants for the oxidative addition and reductive elimination steps, respectively. Similar linear relationships were obtained for iodomethane oxidative addition to complexes **1**, **2** and **4**. The disappearance of the Rh(I) species and formation of the Rh(III)-alkyl^{I} intermediate was monitored

Table 3 UV-Vis kinetic data for the oxidative addition of CH_3I to [Rh(acac)(CO)(PR_3)] complexes at different temperatures in dichloromethane

		Rate Constant				
		$10^3\ k_1/M^{-1}s^{-1}$		$10^3\ k_{-1}/s^{-1}$		
	$T/°C$	IR[a]	UV-Vis	IR[a]	UV-Vis	K_1[b]/M^{-1}
(**1**)	24.9	30.9(3)	30.8(5)	1.0(2)	1.1(2)	27(4)
	15.1		17.2(4)		0.5(1)	31(7)
	5.3		9.71(4)		0.30(1)	33(1)
(**2**)	26.0	52.9(8)	55(1)	1.4(4)	0.9(4)	59(26)[c]
	14.0		27.2(4)		1.2(1)	22(2)
	6.0		18.6(2)		0.64(8)	29(4)
(**3**)	25.6	6.92(4)	6.98(6)	0.07(2)	0.08(2)	90(24)[c]
	14.5		3.38(4)		0.11(2)	31(4)
	5.5		1.88(4)		0.07(2)	27(6)
(**4**)	25.6	26.4(8)	27.1(2)	0.6(4)	0.29(9)	92(29)[c]
	14.3		13.8(2)		0.45(6)	31(4)
	5.9		9.1(1)		0.15(5)	62(20)[c]

[a] IR kinetic data determined at 25 °C. [b] Values calculated for UV-Vis data; $K_1 = k_1/k_{-1}$. [c] Since the intercept indicated a large esd, values should be treated as estimations.

by IR and NMR spectroscopy and gave identical observed rate constants within experimental error. The kinetics as studied by UV/Vis spectroscopy gave similar results (Table 3).

A recent paper of Muller *et al.*[32] reported the oxidative addition of $SeCN^-$ to tertiary phosphine ligands with the corresponding formation of SeP^VR_3. A systematic increase in k_1 for the forward rate of almost 50 times, moving progressively from the weaker electron donating PPh_3 to PCy_3, was observed. This is in agreement with the electronic properties as discussed above and illustrated by both the ν(CO) and $^1J_{Rh-P}$ data, see Table 1. Our results are surprising and do not show the same systematics at all and the steric *vs.* electronic correlation is severely distorted. In fact, the value of k_1 for [Rh(acac)(CO)(**PCyPh$_2$**)] is the highest at $52.9(8) \times 10^{-3}$ $M^{-1}s^{-1}$ and that of [Rh(acac)(CO)(**PCy$_2$Ph**)] is the lowest at $6.92(4) \times 10^{-3}$ $M^{-1}s^{-1}$. The value of k_1 for [Rh(acac)(CO)(**PCy$_3$**)] of $26.4(8) \times 10^{-3}$ $M^{-1}s^{-1}$ is the second slowest, completely opposite to the expected. This could of course be attributed to the fact that there is a metal centre and other ligands with possible inter- and intra-molecular interactions involved in our case.

Clearly, the steric effect by the stepwise introduction of the cyclohexyl group is more subtle and allow also these cyclohexyl groups to utilize its flexibility to assume sterically favourable/or unfavourable conformations, thereby significantly influencing the reactivity at the rhodium(I) centre. Furthermore, the subtle differences in the steric and electronic properties of the tertiary phosphine ligand also shows a significant influence with regard to product formation (see ^{31}P NMR data). The latter observation is however the subject of another study, which also includes significant theoretical calculations on the energies associated with this process.

It is however quite significant that an almost one order-of-magnitude difference is observed from [Rh(acac)(CO)(**PCyPh$_2$**)] to that of [Rh(acac)(CO)(**PCy$_2$Ph**)]. Moreover, as indicated above, it is interesting to note that the Rh–P bond distance obtained from the structural data of [Rh(acac)(CO)(**PCyPh$_2$**)] is the shortest (at 2.2327(6) Å) of the four complexes **1**–**4**, potentially supporting an electron rich rhodium(I) centre (Table 2).

Other examples of manipulating electron density and steric interaction have been explored with [Rh(cacsm)(CO)(PR_3)][5] complexes (cacsmH = cyclohexyl 2-(methylamino)-1-cyclopentene-1-dithiocarboxylato) with different *mono*-dentate phosphine ligands where R = phenyl (Ph), *para*-chlorophenyl (*p*-cPh), *para*-methoxyphenyl (*p*-mPh) and cyclohexyl (Cy). The first three phosphines in this latter series P(*p*-cPh)$_3$, PPh_3 and P(*p*-mPh)$_3$ are sterically virtually identical with the same cone angle[22] of 145°, but have increasing Brønsted pK_a values[33] (1.03, 2.73 and 4.57) indicating an increase in their σ-donating ability. The values for k_1 increased across the series, indicating that the driving factor for the oxidative addition depended on the nucleophilicity of the phosphines. The greater nucleophilicity of the PCy_3 ligand (pK_a = 9.7) suggests that k_1 should be significantly larger than the other three complexes, but it is *ca.* three-four orders of magnitude smaller than the other three complexes. In this case it seemed as if the larger steric demand of the PCy_3 ligand (cone angle = 170°) completely overshadowed the electronic effect.

It is therefore concluded from the current study too that even small changes at or around the metal centre may significantly affect the rate of oxidative addition and therefore the catalytic ability of these types of catalysts, sometimes in orders-of-magnitude. For example Roodt *et al.*[5] varied the ring-size of the bidentate ligand in different [Rh(BID)(CO)(PR_3)] and observed that a small change of *ca.* 10° decrease in bite angle from the six-membered to the five-membered chelates significantly affected the stability of the alkyl intermediate.[5]

However, the significant effect observed in this current study is still quite surprising.

An interesting additional observation concerns the stability constants (K_1) for the formation of the intermediate Rh-alkyl^I species. Although not that convincing due to the large e.s.d.'s of the reductive elimination constants (k_{-1}; Y-intercepts), it seems as if there is not a similar variation in the K_1 values (Table 4). If this had been the case, one would have expected a much larger steric effect on the thermodynamic equilibrium than the virtually independence of the K_1 values shown.

The activation parameters of the [Rh(acac)(CO)(PR_3)] complexes in this study range from 35(3) to 44(1) kJ mol^{-1} for $\Delta H^{\neq}$ and –140(5) to –154(9) J K^{-1} mol^{-1} for $\Delta S^{\neq}$, and the latter in particular, supports an associative activation for the formation of the Rh-alkyl^I (Fig. 8, Table 4).

The significant difference in relative reactivities of the [Rh(acac)(CO)(PR_3)] complexes toward iodomethane oxidative addition is also clearly evident from the Eyring plots shown in Fig. 8.

Table 4 Summary of spectroscopic and kinetic data for the four-coordinated [Rh(acac)(CO)(PR_3)] complexes in solution and associated k_1 values at 25 °C in dichloromethane

	ν(CO)/ cm^{-1}	δ ^{31}P NMR/ppm	$^1J_{Rh-P}$/ Hz	$10^3\ k_1$/ $M^{-1}s^{-1}$	$\Delta H^{\neq}$ (k_1)/ kJ mol^{-1}	$\Delta S^{\neq}$ (k_1)/ J $K^{-1}mol^{-1}$
(**1**)	1977.6	48.6	177.0	30.8(5)	38(1)	–146(4)
(**2**)	1959.3	53.3	171.3	55(1)	35(3)	–152(9)
(**3**)	1948.8	58.8	168.3	6.98(6)	44(1)	–140(5)
(**4**)	1945.3	59.3	164.3	27.1(2)	36(3)	–154(9)

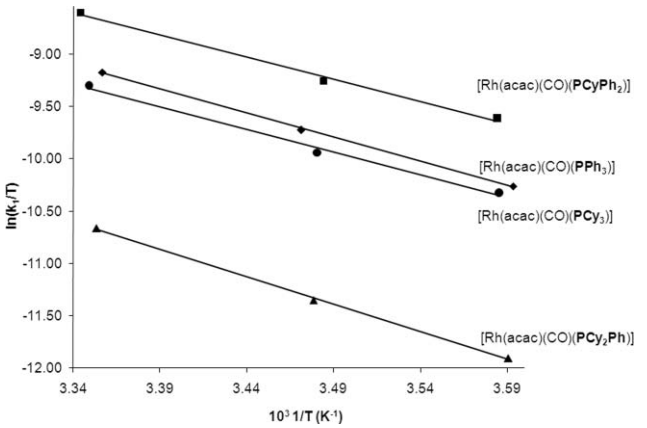

Fig. 8 Eyring plots of the k_1 rate constant (formation of [Rh(acac)I(CH$_3$)(CO)(PR$_3$)]) in CH_2Cl_2.

Conclusion

A systematic study on the effect of gradual substitution of phenyl rings by cyclohexyl groups in rhodium acetylacetonato phosphine complexes is reported. The spectroscopic results show a systematic increase of the electronic and steric effects of the phosphine ligands when moving from complex **1** to **4**. However, the kinetic results of the oxidative addition of CH_3I to these complexes did not follow a systematic pattern. This suggests that very small changes to the steric and electronic properties of Rh(I) complexes and catalysts could significantly (by orders-of-magnitude) affect the behaviour of these systems. A complete computational study of these factors are underway.

Experimental

General procedures

All reagents used for synthesis and characterisation were of analytical grade. If nothing else is stated, all commercially available reagents were used as received from Sigma-Aldrich. All organic solvents were dried and distilled before use. Rhodium trichloride hydrate ($RhCl_3 \cdot xH_2O$) was purchased from Next Chimica, South Africa, and used without further purification.

Synthesis of [Rh(acac)(CO)(PR$_3$)] (1–4)

Tetracarbonyldichloridodirhodium, [Rh(μ-Cl)(CO)$_2$]$_2$, was synthesised according to the method developed by McCleverty and Wilkinson.[34] [Rh(acac)(CO)$_2$] was synthesized by mixing a solution of acetylacetone (0.2 g, 2.2 mmol) in DMF to a similar solution of [Rh(μ-Cl)(CO)$_2$]$_2$ (0.4 g, 1.0 mmol). Upon addition of ice water, the complex precipitated and filtered (0.4 g, 79%). Ligand substitution of the [Rh(acac)(CO)$_2$] complex was performed by dissolving in octane followed by the slow addition of the appropriate PR$_3$ ligand as previously described.[14–16] The mixture was stirred and the light yellow precipitate filtered. Samples suitable for X-ray diffraction were obtained by recrystallization from acetone.

[Rh(acac)(CO)(PPh$_3$)] (1)

Synthesised from [Rh(acac)(CO)$_2$] (50 mg, 0.19 mmol) and free phosphine, PPh$_3$ (56 mg, 0.21 mmol), following general ligand substitution method to yield (**1**) (72 mg, 77%). $\nu_{max}(CH_2Cl_2)/cm^{-1}$ 1977.0 (CO); (neat) 1977.6 (CO); δ_H(300 MHz; $CDCl_3$; Me_4Si) 2.08 (3H, s, Me), 1.60 (3H, s, Me), 5.42 (1H, s, 6-H), 7.66, 7.42, 7.37 (15H, m, Ph); δ_P(121.495 MHz; CH_2Cl_2; H_3PO_4) 48.6 (d, *J* 176.9).

[Rh(acac)(CO)(PCyPh$_2$)] (2)

Synthesised from [Rh(acac)(CO)$_2$] (80 mg, 0.31 mmol) and free phosphine, PCyPh$_2$ (96 mg, 0.35 mmol), following general ligand substitution method to yield (**2**) (102 mg, 66%). $\nu_{max}(CH_2Cl_2)/cm^{-1}$ 1971.2 (CO); (neat) 1959.3 (CO); δ_H(300 MHz; $CDCl_3$; Me_4Si) 2.05 (3H, s, Me), 1.77 (3H, s, Me), 5.44 (1H, s, 6-H), 7.72, 7.39 (10H, m, Ph), 1.75–1.12, 2.72 (11H, m, Cy); δ_P(121.495 MHz; CH_2Cl_2; H_3PO_4) 53.3 (d, *J* 171.3).

[Rh(acac)(CO)(PCy$_2$Ph)] (3)

Synthesised from [Rh(acac)(CO)$_2$] (62 mg, 0.24 mmol) and free phosphine, PCy$_2$Ph (73 mg, 0.26 mmol), following general ligand substitution method to yield (**3**) (97 mg, 80%). $\nu_{max}(CH_2Cl_2)/cm^{-1}$ 1967.4 (CO); (neat) 1948.8 (CO); δ_H(300 MHz; $CDCl_3$; Me_4Si) 2.09 (3H, s, Me), 1.81 (3H, s, Me), 5.46 (1H, s, 6-H), 7.79, 7.39 (5H, m, Ph), 1.70–1.14, 2.41 (22H, m, Cy); δ_P(121.495 MHz; CH_2Cl_2; H_3PO_4) 58.8 (d, *J* 168.3).

[Rh(acac)(CO)(PCy$_3$)] (4)

Synthesised from [Rh(acac)(CO)$_2$] (52 mg, 0.20 mmol) and free phosphine, PCy$_3$ (62 mg, 0.22 mmol), following general ligand substitution method to yield (**4**) (91 mg, 89%). $\nu_{max}(CH_2Cl_2)/cm^{-1}$ 1959.7 (CO); (neat) 1945.3 (CO); δ_H(300 MHz; $CDCl_3$; Me_4Si) 2.05 (3H, s, Me), 1.86 (3H, s, Me), 5.43 (1H, s, 6-H), 2.11, 1.99, 1.83–1.26 (33H, m, Cy); δ_P(121.495 MHz; CH_2Cl_2; H_3PO_4) 59.3 (d, *J* 164.3).

X-ray diffraction analysis

The reflection data were collected on a Bruker X8 Apex II 4 K Kappa CCD diffractometer with APEX2 software[35] utilizing COSMO[36] for optimum collection of more than a hemisphere of reciprocal space. The frames were integrated using a narrow-frame integration algorithm and reduced with the Bruker SAINT-PLUS[37] and XPREP[37] software packages. Data were corrected for absorption effects using the multi-scan technique SADABS.[38] The structure was solved by the direct methods package SIR97[39] and refined using the WINGX software package[40] incorporating SHELXL.[41] The program DIAMOND[42] was used for all graphical representation of the crystal structures. All structures are shown with thermal ellipsoid drawn at 50% probability level.

Kinetic measurements

The oxidative addition of iodomethane to complexes **1** to **4** were monitored by repetitive IR and ^{31}P NMR scans at 25 °C. IR spectra were recorded on a Digilab FTS 2000 Fourier transform spectrometer utilizing a He–Ne laser at 632.6 nm equipped with a

temperature cell regulator (± 0.3 °C). UV-Vis kinetic measurements were conducted on a Varian Cary 50 Conc. spectrometer equipped with a Julabo F12-mV temperature cell regulator (accurate within 0.1 °C) in a 1.00 cm quartz tandem cuvette cell. Temperature variations for UV-Vis kinetic experiments were performed between 5 and 25 °C. The ^{31}P NMR spectra were obtained on a Bruker AXS300 spectrometer at 25 °C. ^{31}P chemical shifts are reported relative to 85% H_3PO_4 (0 ppm) as external standard; positive shifts are downfield. The observed first-order rate constants were obtained from least-squares fits of absorbance *versus* time data, under pseudo-first order conditions, with $[Rh]_{tot.} = 1 \times 10^{-4}$ M. All kinetic measurements were conducted in dichloromethane unless otherwise indicated.

Acknowledgements

Financial assistance from the South African National Research Foundation (NRF), THRIP, SASOL, and Research Fund of the University of the Free State is gratefully acknowledged. Part of this material is based on work supported by the South African National Research Foundation (GUN 2038915). Opinions, findings, conclusions or recommendations expressed in this material are those of the authors and do not necessarily reflect the views of the NRF.

Notes and references

1 P. M. Maitlis, A. Haynes, G. J. Sunley and M. J. Howard, *J. Chem. Soc., Dalton Trans.*, 1996, 2187.
2 P. W. N. M. van Leeuwen, in *Homogeneous Catalysis: Understanding the Art*, Kluwer Academic Publishers, Dordrecht, 2004, ch. 6, pp. 109–124.
3 S. S. Basson, J. G. Leipoldt, A. Roodt, J. A. Venter and T. J. Van Der Walt, *Inorg. Chim. Acta*, 1986, **119**, 35.
4 K. G. van Aswegen, J. G. Leipoldt, I. M. Potgieter, G. J. Lamprecht, A. Roodt and G. J. van Zyl, *Transition Met. Chem.*, 1991, **16**, 369.
5 A. Roodt and G. J. J. Steyn, *Recent Res. Devel. Inorganic Chem.*, 2000, **2**, 1.
6 G. J. J. Steyn, A. Roodt, I. Poletaeva and Y. S. Varshavsky, *J. Organomet. Chem.*, 1997, **536–537**, 197.
7 Y. S. Varshavsky, T. G. Cherkasova, N. A. Buzina and L. S. Bresler, *J. Organomet. Chem.*, 1994, **464**, 239.
8 S. S. Basson, J. G. Leipoldt, A. Roodt and J. A. Venter, *Inorg. Chim. Acta*, 1987, **128**, 31.
9 J. G. Leipoldt, S. S. Basson and L. J. Botha, *Inorg. Chim. Acta*, 1990, **168**, 215.
10 C. H. Cheng, B. D. Spivack and R. Eisenberg, *J. Am. Chem. Soc.*, 1977, **99**, 3003.
11 G. J. J. Steyn, A. Roodt and J. G. Leipoldt, *Inorg. Chem.*, 1992, **31**, 3477.
12 J. Conradie, G. J. Lamprecht, A. Roodt and J. C. Swarts, *Polyhedron*, 2007, **26**, 5075.
13 J. G. Leipoldt, S. S. Basson, L. D. C. Bok and T. I. A. Gerber, *Inorg. Chim. Acta*, 1978, **26**, L35.
14 A. M. Trzeciak, B. Borak, Z. Ciunik, J. J. Ziółkowski, M. F. C. Guedes da Silva and A. J. L. Pombeiro, *Eur. J. Inorg. Chem.*, 2004, 1411.
15 A. Brink, A. Roodt and H. G. Visser, *Acta Crystallogr., Sect. E: Struct. Rep. Online*, 2007, **63**, m2831.
16 A. Brink, A. Roodt and H. G. Visser, *Acta Crystallogr., Sect. E: Struct. Rep. Online*, 2006, **63**, m48.
17 A. M. Trzeciak and J. J. Ziółkowski, *Inorg. Chim. Acta*, 1985, **96**, 15.
18 W. Simanko, K. Mereiter, R. Schmid, K. Kirchner, A. M. Trzeciak and J. J. Ziółkowski, *J. Organomet. Chem.*, 2000, **602**, 59.
19 A. M. Trzeciak, T. Głowiak, R. Grzybek and J. J. Ziółkowski, *J. Chem. Soc., Dalton Trans.*, 1997, 1831.
20 S. Otto, A. Roodt and J. Smith, *Inorg. Chim. Acta*, 2000, **303**, 295.
21 G. Ferguson, P. J. Roberts, E. C. Alyea and M. Khan, *Inorg. Chem.*, 1978, **17**, 2965.
22 C. A. Tolman, *Chem. Rev.*, 1977, **77**, 313.
23 K. G. van Aswegen, J. G. Leipoldt, I. M. Potgieter, G. J. Lampecht, A. Roodt and G. J. van Zyl, *Transition Met. Chem.*, 1991, **16**, 369.
24 A. Elduque, Y. Gareés, L. A. Oro, M. T. Pinillos, A. Tiripicchio and F. Ugozzoli, *J. Chem. Soc., Dalton Trans.*, 1996, 2155.
25 L. J. Damoense, *Ph.D. Thesis*, University of the Free State, 2000.
26 Y. S. Varshavsky, M. R. Galding, T. G. Cherkasova, I. S. Podkorytov, A. B. Nikol'skii, A. M. Trzeciak, Z. Olejnik, T. Lis and J. J. Ziólkowski, *J. Organomet. Chem.*, 2001, **628**, 195.
27 M. Cano, J. V. Heras, M. A. Lobo, E. Pinilla and M. A. Monge, *Polyhedron*, 1992, **11**, 2679.
28 L. J. Damoense, W. Purcell and A. Roodt, *Rhodium Express*, 1995, **14**, 4.
29 G. Steyl, *Polyhedron*, 2007, **26**, 5324.
30 G. Steyl. *Ph.D. Thesis*, Rand Afrikaans University, 2004.
31 M. M. Conradie and J. Conradie, *Inorg. Chim. Acta*, 2009, **362**, 519.
32 A. Muller, S. Otto and A. Roodt, *Dalton Trans.*, 2008, 650.
33 C. A. McAuliffe, in *Comprehensive Coordination Chemistry*, ed. G. Wilkinson, R.D. Gillard and J.A. McCleverty, Pergamon Press, Oxford, 1st edn, 1987, vol. 2, ch. 14, pp. 989–1037.
34 J. A. McCleverty and G. Wilkinson, *Inorg. Synth.*, 1990, **28**, 84.
35 APEX2 (Version 1.0-27), Bruker AXS Inc., Madison, Wisconsin, USA, 2005.
36 COSMO, Version 1.48, Bruker AXS Inc., Madison, Wisconsin, USA, 2003.
37 SAINT-PLUS, Version 7.12 (including XPREP), Bruker AXS Inc., Madison,Wisconsin, USA, 2004.
38 SADABS, Version 2004(1), Bruker AXS Inc., Madison, Wisconsin, USA, 1998.
39 A. Altomare, M. C. Burla, M. Camalli, G. L. Cascarano, C. Giacovazzo, A. Guagliardi, A. G. G. Moliterni, G. Polidori and R. Spagna, *J. Appl. Crystallogr.*, 1999, **32**, 115.
40 L. J. Farrugia, *J. Appl. Crystallogr.*, 1999, **32**, 837.
41 G. M. Sheldrick, *SHELXL97 Program for Crystal Structure Refinement*, University of Göttingen, Germany, 1997.
42 K. Brandenburg and H. Putz, *DIAMOND*, Release 3.1a. Crystal Impact GbR, Bonn, Germany, 2005.

